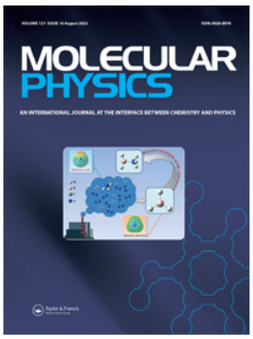

Taylor & Francis
Taylor & Francis Group

Molecular Physics

An International Journal at the Interface Between Chemistry and Physics

ISSN: (Print) (Online) Journal homepage: https://www.tandfonline.com/loi/tmph20

Vibrationally- and rotationally-resolved photoelectron imaging of cryogenically-cooled SbO_2^-

G. Stephen Kocheril, Han-Wen Gao & Lai-Sheng Wang

To cite this article: G. Stephen Kocheril, Han-Wen Gao & Lai-Sheng Wang (2023): Vibrationally- and rotationally-resolved photoelectron imaging of cryogenically-cooled SbO_2^-, Molecular Physics, DOI: 10.1080/00268976.2023.2182610

To link to this article: https://doi.org/10.1080/00268976.2023.2182610

MOLECULAR PHYSICS e2182610
https://doi.org/10.1080/00268976.2023.2182610

Taylor & Francis
Taylor & Francis Group

FESTSCHRIFT IN MEMORY OF DIETER GERLICH SPECIAL ISSUE

Vibrationally- and rotationally-resolved photoelectron imaging of cryogenically-cooled SbO_2^-

G. Stephen Kocheril, Han-Wen Gao and Lai-Sheng Wang

Department of Chemistry, Brown University, Providence, RI, USA

ABSTRACT

We report a temperature-controlled photoelectron imaging study of SbO_2^-, produced from a laser vaporisation source and cooled in a cryogenic 3D Paul trap. Vibrationally resolved photoelectron spectra are obtained for the ground state detachment transition, yielding the bending frequencies for both SbO_2 and SbO_2^-. Franck-Condon simulations also allow the estimate of the vibrational temperature of the trapped SbO_2^- anion. A near-threshold spectrum of SbO_2^- at a photon energy of 3.4958 eV reveals partially resolved rotational structure for the 0–0 transition, which yields an accurate electron affinity of 3.4945 ± 0.0004 eV for SbO_2. The rotational simulation also yields an estimated rotational temperature of the trapped ions.

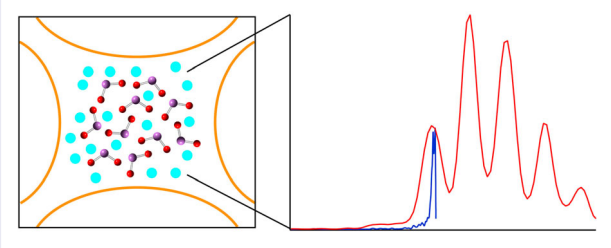

ARTICLE HISTORY
Received 28 December 2022
Accepted 15 February 2023

KEYWORDS
Photoelectron imaging; cryogenic cooling; ion traps; photoelectron spectroscopy; antimony oxide

1. Introduction

Internally cold molecules are critical for high resolution molecular spectroscopy. Over the past two decades, cryogenically cooled ion traps have significantly advanced ion spectroscopy by providing a reliable and robust method to control the rotational and vibrational temperatures of molecular ions. First introduced by Prof. Dieter Gerlich [1], cryogenically cooled linear ion traps have been widely adapted for the spectroscopy of ionic species. In particular, the celebrated 22-pole ion trap has been used to great success in carrying out rotational spectroscopy [2], infrared photodissociation [3], and electronic spectroscopy [4,5] on a wide variety of molecular cations. Our lab first developed a cryogenically-cooled 3D Paul trap for photoelectron spectroscopy (PES) of negative ions produced from electrospray ionisation (ESI) [6,7]. This technique demonstrated the importance of cooling large molecular ions in PES studies as the reduction of vibrational hot bands led to well-resolved spectra even for large fullerene anions [8–11]. A cryogenically cooled octupole ion trap has been coupled with slow electron velocity-map imaging (VMI) for high resolution PES studies of molecular ions [12,13]. The 3D Paul trap is convenient to implement and conducive to ion extraction and subsequent mass analyses [7]. We have coupled a cryogenically-cooled ion trap with an ESI ion source and a VMI system to conduct high-resolution PES (ESI-PES) of complex molecular anions [14–16]. Very recently we have constructed a new cryogenic Paul trap that is integrated to a laser vaporisation cluster source and a VMI system aimed to investigate size-selected clusters [17].

The first experiment that we conducted on the new apparatus was a high resolution vibrationally-resolved photoelectron imaging of BiO_2^-, measuring the vibrational frequencies and electron affinity (EA) of BiO_2 for the first time [17]. Surprisingly, among the group 15

CONTACT Lai-Sheng Wang lai-sheng_wang@brown.edu Department of Chemistry, Brown University, Providence, RI 02912, USA

Supplemental data for this article can be accessed here. https://doi.org/10.1080/00268976.2023.2182610

dioxides (MO_2), only NO_2^- [18] and PO_2^- [19] have been studied by PES previously, in addition to our recent study on the heaviest member of this series. There have been no experimental studies on either AsO_2^- or SbO_2^-. In the current article, we focus on the study of SbO_2^- in our continued effort to debug and tune our recently constructed cryogenic trap laser vaporisation VMI apparatus. Interestingly, the SbO_2 molecule was the subject of a series of theoretical investigations by Lee *et al*., who studied its structures and electronic properties in all its three charge states [20–22]. In particular, they computed the EA of SbO_2 and predicted the photoelectron spectrum of SbO_2^- to the first three electronic states of SbO_2 [22]. However, there have been no experimental results to compare with these computational data. The only prior experiment was a chemiluminescence observation of SbO_2 formed from reactions between Sb and O_3, but no specific spectroscopic information was obtained [23].

In the current study, we report vibrationally resolved photoelectron spectra for the ground state detachment transition of cryogenically-cooled SbO_2^-. A broad vibrational progression is observed mainly due to the bending mode (ν_2) of SbO_2. A near threshold photoelectron spectrum yields a rotationally resolved 0–0 transition and an accurate EA of 3.4945 ± 0.0004 eV for SbO_2. The bending frequencies for SbO_2 and SbO_2^- are measured to be $194 \pm 3\,cm^{-1}$ and $285 \pm 10\,cm^{-1}$, respectively. Both the vibrational and rotational temperatures are estimated from Franck-Condon (FC) and rotational simulations, respectively. Our results are consistent with the previous theoretical calculations, which slightly overestimated both the EA of SbO_2 and the structure changes from the anion to the neutral.

2. Experimental methods

The experiments were carried out on our recently developed laser-vaporisation based high-resolution photoelectron imaging apparatus equipped with a temperature-controlled Paul trap [17]. Briefly, the second harmonic of a Nd:YAG laser was focused onto a solid disk target of antimony (99.8%, Alfa Aesar). The laser-induced plasma was quenched by a high pressure He carrier gas seeded with 1% O_2 to promote formation of antimony oxide clusters. Nascent clusters were entrained by the carrier gas and underwent a supersonic expansion. After passing a skimmer, anions in the collimated beam were sent directly into a cryogenically-cooled 3D Paul trap. The ion trap was cooled down to 4.1 K by a two-stage closed-cycle helium refrigerator and could be controlled up to 300 K. The trapped anions were collisionally cooled by a mixed He/H_2 buffer gas (19:1 by volume) for 45 ms before being pulsed into the extraction zone of a time-of-flight (TOF) mass spectrometer. The radio frequency (RF) voltage on the Paul trap was adjusted to optimise trapping efficiency. Since there are two stable isotopes for Sb (121 and 123), the more intense $^{121}SbO_2^-$ anion was mass-selected before entering the interaction zone of the VMI spectrometer. Photodetachment was performed using the third harmonic of an injection seeded Nd:YAG laser (Continuum Powerlite 9020, 354.67 nm, 3.4958 eV) and a frequency-doubled Nd:YAG-pumped tunable dye laser. Photoelectrons were extracted and focused onto a set of microchannel plates coupled to a phosphor screen and charge-coupled device camera. Raw images were acquired for 100,000–250,000 laser shots and were processed using the maximum entropy Legendre expansion method (MELEXIR) [24]. The VMI lens was calibrated using photoelectron images of Au^- and Bi^- at various photon energies. The typical kinetic energy (Ke) resolution of our VMI system was $\sim$0.6% (ΔKe/Ke) for fast electrons (>1 eV) and as low as $1.2\,cm^{-1}$ for very slow electrons [25].

Uncertainties for individual peaks were estimated using their full width at half maximum. The uncertainties for specific vibrational frequencies were estimated after taking the average of a given vibrational progression and considering the deviations between the peaks. The average uncertainty for a vibrational mode was further evaluated from the FC simulations, which were used to guide the spectral assignment of the resolved vibrational progression.

Photoelectron angular distributions (PADs) were obtained from the images, characterised by the anisotropy parameter (β). The differential cross section of photoelectrons from unoriented targets can be expressed as:

$$d\sigma/d\Omega = \sigma_{Tot}/4\pi\,[1 + \beta P_2(cos(\theta)] \qquad (1)$$

where σ_{Tot} is the total cross section, P_2 is the second-order Legendre polynomial, and θ is the angle of the photoelectron relative to the laser polarisation. Hence, the PAD is described by:

$$I(\theta) \sim [1 + \beta P_2(cos(\theta)] \qquad (2)$$

where β has a value ranging from -1 to 2 [26]. This model works well for single photon detachment transitions from randomly oriented molecules. As photons carry one unit of angular momentum, the angular momentum of the outgoing photoelectron will be $l = \pm 1$. If an electron is detached from an s atomic orbital ($l = 0$), the outgoing photoelectron will have $l = 1$ (pure p-wave) with $\beta = 2$. It is non-trivial to interpret the β-value for electron detachment from molecular orbitals (MOs) since MOs are linear combinations

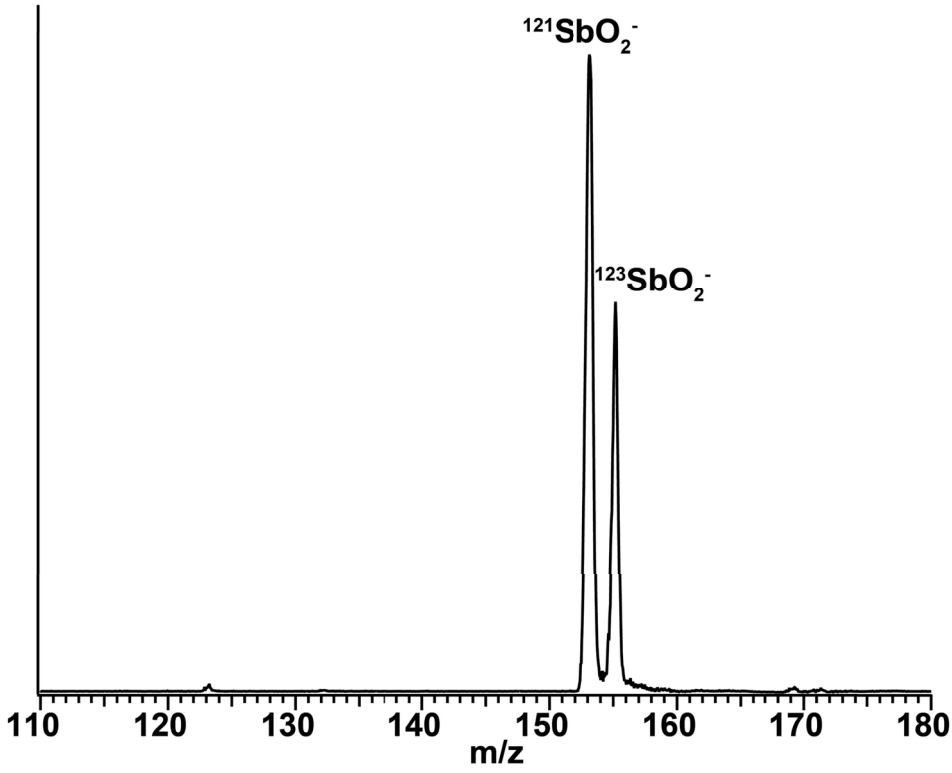

Figure 1. Mass spectrum of the SbO_2^- anion produced by laser vaporisation and cooled in a 3D Paul trap held at 4.1 K, using an RF voltage of 300 V.

of atomic orbitals. Nevertheless, the values of β can be used to qualitatively assess the symmetries of the MOs involved in the photodetachment process and provide valuable electronic information [27].

3. Results

As shown previously [17], the addition of the 3D Paul trap before the TOF mass analysis alters the observable cluster distribution from the laser vaporisation cluster source. This occurs because the trapping efficiency for a given mass displays some dependence on the RF voltage applied to the Paul trap. For the current experiment, we optimised the mass spectrum for a small mass range centred around SbO_2^-. Figure 1 shows the mass spectrum with a RF voltage of 300 V and the Paul trap operated at 4.1 K. Two intense peaks were observed, corresponding to the ^{121}Sb and ^{123}Sb isotopes of SbO_2^-. Surprisingly, no Sb^- or SbO^- anions were observed; only very weak signals of SbO_3^- were discernible at m/z of 169 and 171. This observation implies that the SbO_2^- anion is particularly stable and it is formed very efficiently in our laser vaporisation source.

Photoelectron images and spectra of SbO_2^- were obtained at three different photon energies, as shown in Figure 2, with the ion trap operated at 4.1 K. A broad vibrational progression was observed, suggesting a large geometry change between the ground state of the anion and that of neutral SbO_2. The RF voltage used for the Paul trap was varied in each experiment to maximise the number of ions probed by the photodetachment laser. Typically, a lower RF voltage indicates a lower q-value on the trap [28], which yields colder trapped ions. The threshold spectrum in Figure 2a represents the coldest condition with RF = 250 V, evidenced by the negligible vibrational hot band. The spectra shown Figure 2b and c were taken at a RF voltage of 300 V, which represents a warmer condition, as evidenced by an observable vibrational hot band (labelled 'hb').

The 0–0 transition (peak X) observed in the near threshold spectrum at 3.4958 eV was found to contain fine features due to partially resolved rotational structures (see the inset of Figure 2a). This high resolution spectrum defines an accurate EA of 3.4945 ± 0.0004 eV for SbO_2 from comparison with rotational simulations (*vide infra*). The resolved peaks (*a*–*h*) represent vibrational excitations of SbO_2. Peak *a* defines a vertical detachment energy (VDE) of 3.52 eV from the SbO_2^- anion to the neutral SbO_2 ground state. The angular distribution displays a clear p-partial wave for the outgoing electrons, suggesting the highest occupied molecular orbital (HOMO) of SbO_2^- is a σ-type orbital.

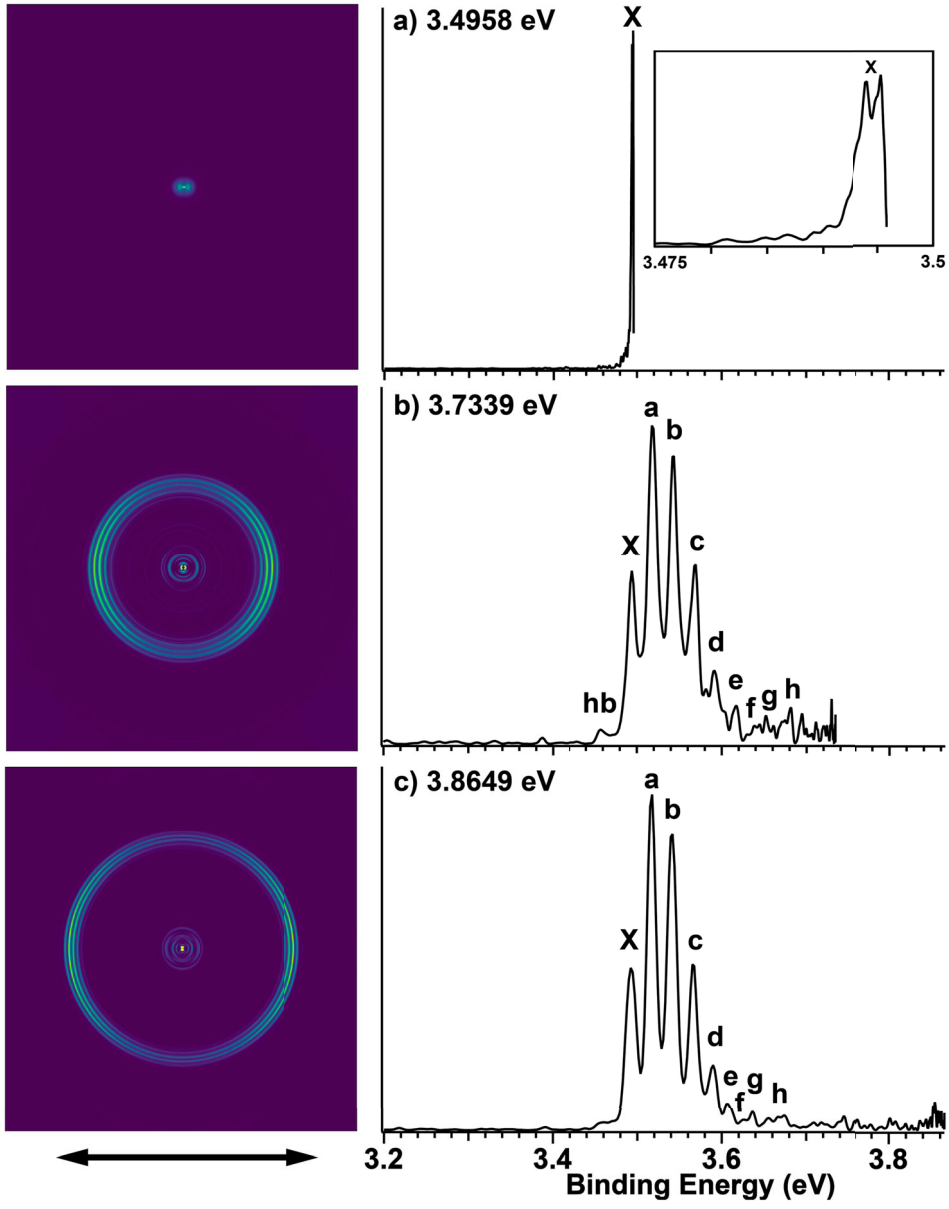

Figure 2. Photoelectron images and spectra of SbO_2^- at a) 3.4958 eV (RF = 250 V), b) 3.7339 eV (RF = 300 V), and c) 3.8649 eV (RF = 300 V). The double arrow below the images indicates the laser polarisation.

The binding energies of all the resolved vibrational features, the anisotropy parameter (β), and assignments are given in Table 1. All the listed β parameters were determined from the image shown in Figure 2c, as it was the highest photon energy used in this study.

4. Discussion

4.1. The electronic structure of SbO_2^-

The high stability SbO_2^- is due to its closed shell nature, as confirmed by its large adiabatic detachment energy of 3.4945 eV or the EA of SbO_2. The calculations by Lee *et al.* [22] predicted an EA ranging from 3.54–3.64 eV, depending on the theoretical methods used, in good agreement with our experimental measurement. The clear *p*-wave detachment, corresponding to a positive β value (Table 1) agrees well with the σ-type HOMO of SbO_2^- calculated at the B3LYP/aug-cc-pVTZ level with an effective core potential on Sb using Gaussian 09 (Figure 3). The HOMO describes weak anti-bonding interactions between the Sb atom and the O atoms and bonding interactions between the two O atoms. Thus, it is expected that the neutral ground state of SbO_2 upon the removal of a HOMO electron from SbO_2^- should have two slightly shorter Sb–O bonds and a larger ∠OSbO bond angle. Indeed, at their highest level of

Table 1. The observed binding energies of vibrational peaks, their β values and assignments from the photoelectron spectra of SbO_2^- in Figure 2.

Peak	Assignment	Binding Energy (eV)	β [a]
hb	2_1^0	3.46(1)	0.63
X	0_0^0	3.4945(4)	0.82
a	2_0^1	3.52(1)	0.61
b	2_0^2	3.54(1)	0.56
c	2_0^3	3.57(1)	0.54
d	1_0^1	3.59(1)	0.71
e	$1_0^1 2_0^1$	3.61(1)	0.71
f	3_0^2	3.63(1)	0.53
g	$1_0^1 2_0^2$	3.65(1)	–
h	$1_0^1 3_0^2$	3.67(1)	–

[a] In cases where the intensity of a transition was too low, the β parameter could not be evaluated.

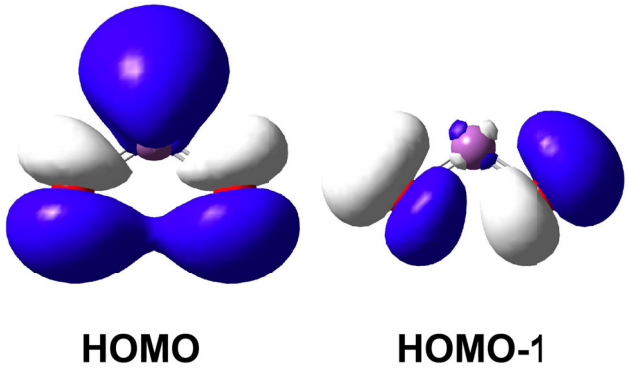

Figure 3. The HOMO (a_1) and HOMO-1 (b_2) of SbO_2^- (isovalue = 0.02 e/bohr^3).

theory [RCCSD(T)/E], Lee *et al.* predicted a Sb–O bond length of 1.8482 Å and a ∠OSbO bond angle of 111.19° for the ground state of SbO_2^- ($^1A_1$) [22] and a Sb–O bond length of 1.8271 Å and a ∠OSbO bond angle of 121.75° for the ground state of SbO_2 ($^2A_1$) [21].

The first excited state of SbO_2 ($^2B_2$) was predicted to appear around 3.76–3.82 eV by Lee *et al.* [22]. We did not observe clear features that could be attributed to this excited state in the spectrum taken at 3.8649 (Figure 2c). The previous calculation predicted a very large ∠OSbO bond angle reduction to 88° in the $^2B_2$ excited state and a very broad FC envelope with a VDE of 4.1 eV in the simulated photoelectron spectrum. Our experimental result is consistent with the theoretical prediction because the computed FC factors for the first few vibrational levels of the detachment transition to the $^2B_2$ excited state were very small.

4.2. Franck-condon simulation

The vibrational progression observed in our photoelectron spectra is expected to involve the bending mode (ν_2) of SbO_2 because of the large bond angle change from the ground state of SbO_2^- to that of SbO_2, as discussed above. The vibrational frequency of 194 ± 3 cm^{-1} measured from our photoelectron spectra is in good agreement with the computed ν_2 frequency of 205.1 cm^{-1} [22], as shown in Table 2. The calculated photoelectron spectrum for the ground state detachment transition by Lee *et al.* was done at room temperature with considerable hot band transitions. Furthermore, their predicted geometry changes appeared to be larger than our photoelectron spectra suggest. The VDE is defined by the binding energy of the maximum v = 1 peak to be 3.52 ± 0.01 eV, whereas Lee *et al.* predicted a maximum at v = 2.

We simulated the FC profile of the ground state detachment transition using the ezFCF programme [29] and the previous theoretical results as the starting point. The FC simulation can only provide changes in the bond length or bond angle. In the current case, we used the computed anion geometry from Lee *et al.* [22] because it was likely to be more accurate due to the closed-shell nature of SbO_2^-. During the simulation, the neutral bond length, bond angle, and the vibrational temperature of the anion were manually adjusted until a satisfactory fit to the experiment was achieved, as shown in Figure 4. The simulation yielded a bond length change of −0.020 Å and a bond angle change of +8.70° from the anion to the neutral ground state. These correspond to a Sb–O bond length of 1.828 Å and a neutral bond angel of 119.89° (Table 2), which are in good agreement with the prediction be Lee *at el.* [21]. Apparently, the neutral bond angle was overestimated in the calculations by Lee *et al.* We found that the FC profile was very sensitive to the bond angle. The FC simulation suggested that the ν_1 mode was also excited, in agreement with the slight Sb–O bond length change, though not clearly resolved in our experiment due to overlap with the v = 4 level of the bending mode. Due to the overlapping spectral features, the FC simulation was used primarily to determine the vibrational frequencies. The obtained ν_1 frequency of 768 ± 7 cm^{-1} is in good agreement with the computed frequency of 762.4 cm^{-1} (Table 2). The weak hot band also yielded a ν_2 frequency of 285 ± 10 cm^{-1} for the SbO_2^- anion, compared with the computed frequency of 263.9 cm^{-1} (Table 2). The asymmetric ν_3 mode is symmetry-forbidden, and only even quanta of the ν_3 mode are allowed upon photodetachment. Because of the small FC factors and spectral congestion, the high binding energy side of the FC profile (Figure 2) was not well resolved. The assignment of ν_3 related levels in Table 1 is therefore tentative.

The FC simulation yielded an anion vibrational temperature of 80 ± 10 K. This temperature is consistent with the vibrational temperature of BiO_2^- that we obtained recently [17]. However, it is higher than what we expected relative to the rotational temperature we were able to

Table 2. Summary of the derived molecular properties for SbO_2^- and SbO_2.

	Experimental		Theoretical [22]	
	SbO_2^- ($^1A_1$)	SbO_2 ($^2A_1$)	SbO_2^- ($^1A_1$)	SbO_2 ($^2A_1$)
ν_1 (cm^{-1})	–	768 ± 7	764.7	762.4
ν_2 (cm^{-1})	285 ± 10	194 ± 3	263.9	205.1
Δr_e (Å)	−0.020 [anion (1.848) → neutral (1.828)]		1.8482	1.8277
$\Delta\theta$ (°)	+8.70 [anion (111.19) → neutral (119.89)]		111.19	121.87

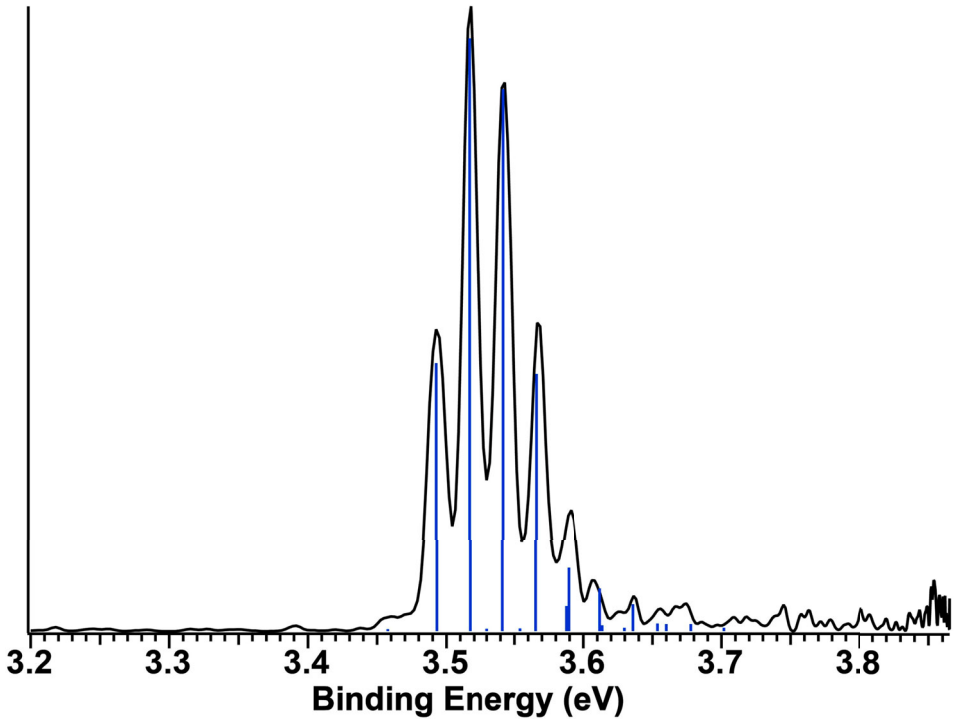

Figure 4. Franck-Condon simulation for the ground state detachment transition of SbO_2^- at 80 K, overlayed with the observed spectrum.

obtain for organic molecular anions from our third-generation ESI-PES apparatus [30–32]. This observation demonstrates the importance of tuning the RF voltage on the Paul trap and its impact on the final anion temperature. As well known in ion-trap mass spectrometry [28], ion temperatures in the Paul trap depend on the q-value, which is directly related to the RF voltage. A large q-value (large RF voltage) results in less effective cooling or even RF heating. By varying the RF voltage or the q-value, we are able to tune the temperature of the trapped ions, while balancing the trapping efficiency. The spectra shown in Figure 2b and c using RF = 300 V exhibit a relatively high vibrational temperature of 80 K, while the spectrum in Figure 2a using RF = 250 V indicates significantly colder anions since the hot band population is negligible. However, a larger RF amplitude was necessary at the higher photon energies in order to increase the trapping efficiency to allow data acquisition in a reasonable time frame due to the low detachment photon flux from the frequency-doubled dye laser output.

4.3. Rotational simulation

The spectrum taken at 3.4958 eV revealed partially resolved rotational structure for the SbO_2 final state (inset of Figure 2a). This observation allowed us to estimate the rotational temperature of SbO_2^- in the Paul trap. A rotational simulation was preformed using PGOPHER [33]. Initially, the simulation was performed using the geometric parameters obtained from the FC simulation above, i.e. the calculated anion geometry [22] and our derived neutral geometry given in Table 2. These structures, i.e. rotational constants, were manually adjusted in an attempt to fit the observed spectrum using a Gaussian linewidth of 2 cm^{-1} and varying the temperature from 10 to 150 K. The resulting simulated rotational contour is shown in Figure 5, using a band origin of

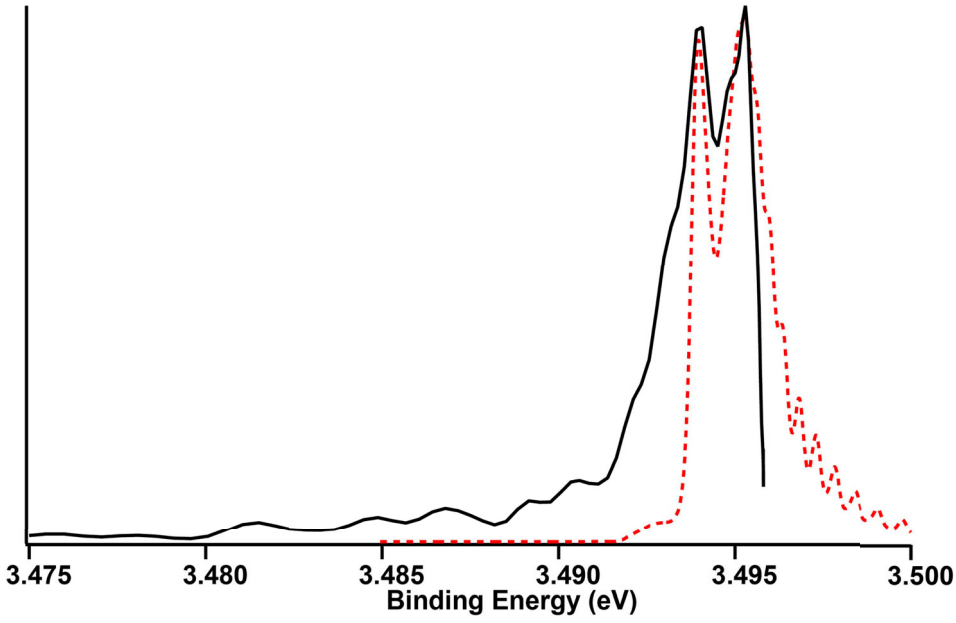

Figure 5. The photoelectron spectrum of SbO_2^- at 3.4958 eV (solid line) compared with rotational simulation for a *b*-type transition (dashed line).

Table 3. Rotational constants used from in the rotational profile simulation.

	SbO_2^- ($^1A_1$)	SbO_2 ($^2A_1$)
A (MHz)	6595.99	6310.64
B (MHz)	18142.74	23835.25
C (MHz)	4837.33	4989.59

3.4945 eV, with the associated rotational constants given in Table 3. This simulation yielded a rotational temperature of 70 ± 20 K, which is similar to the vibrational temperature obtained in the FC simulation at a larger *q*-value of the ion trap. The simulation suggests that the photon energy of 3.4958 eV cut off part of the R branch for the 0–0 transition, preventing a definitive fit for both the rotational constants and temperature using PGOPHER. The 70 K rotational temperature is significantly higher than the 30 K rotational temperature that we estimated for organic anions studied using our third-generation ESI-PES apparatus [30–32]. One possibility could be that the rotational cooling is less effective for the smaller system relative to the larger organic anions. Another possibility was due to the inaccurate rotational constants used in the simulation because clearly the simulation is not in perfect agreement with the experimental spectrum. Furthermore, the rotational simulation for the photoelectron spectrum is intrinsically more challenging because accurate rotational constants are required for both the anion initial state and the neutral final state.

5. Conclusion

We report the first photoelectron imaging study on SbO_2^- which was produced from a laser vaporisation source and cooled in a cryogenically-controlled ion trap. Extensive vibrational fine structures were observed for the ground state detachment transition, as well as rotational fine structures for the 0–0 transition in a near-threshold photoelectron spectrum. The electron affinity of SbO_2 was measured accurately to be 3.4945 ± 0.0004 eV. The vibrational frequencies for the bending mode of both SbO_2 and SbO_2^- were measured to be 194 ± 3 cm^{-1} and 285 ± 10 cm^{-1}, respectively. Franck-Condon simulations yielded accurate bond length and bond angle changes from the anion to the neutral ground state of SbO_2, as well as an estimate of the vibrational temperature of SbO_2^- (∼80 K). The rotational simulation also yielded a similar rotational temperature for the trapped SbO_2^- anion.

Acknowledgements

This paper is dedicated to the memory of Prof. Dieter Gerlich. One of us (PI: L.S.W.) would like to thank Prof. Dieter Gerlich for his support and discussion when he was developing the first cryogenically-cooled 3D Paul trap [6,7]. When the PI was preparing the design of this instrument, he invited Dieter to Richland, Washington for consultation. Much to his surprise, Dieter told him that the 3D Paul trap would not work and instantly offered the PI his 22-pole ion trap design! After the PI realised that the dimension of Dieter's 22-pole ion trap was similar to the commercially available Paul trap, he went ahead

with his original plan, reasoning that if it did not work he could easily switch to the 22-pole trap design. Dieter even connected the PI to have a decommissioned 22-pole ion trap from Taiwan shipped to the PI then at Richland, Washington, which was eventually shipped back to Dieter in Germany after the 3D Paul trap design was shown to be effective in cooling trapped ions from an electrospray ion source [6–11].

Disclosure statement

No potential conflict of interest was reported by the author(s).

Funding

This work was supported by the National Science Foundation(NSF) under Award No. CHE-2053541. GSK was partially supported by a NASA Rhode Island Space Science Grant Award No. 80NSSC20M0053.

ORCID

G. Stephen Kocheril http://orcid.org/0000-0003-1388-6472
Lai-Sheng Wang http://orcid.org/0000-0003-1816-5738

References

[1] D. Gerlich, Adv. Chem. Phys. **82**, 1 (1992).
[2] O. Asvany and S. Schlemmer, Phys. Chem. Chem. Phys. **23**, 26602 (2021). doi:10.1039/D1CP03975J
[3] P. Jusko, S. Brünken, O. Asvany, S. Thorwirth, A. Stoffels, L. van der Meer, G. Berden, B. Redlich, J. Oomens and S. Schlemmer, Faraday Discuss. **217**, 172 (2019). doi:10.1039/C8FD00225H
[4] T.R. Rizzo, J.A. Stearns and O.V. Boyarkin, Int. Rev. Phys. Chem. **28**, 481 (2009). doi:10.1080/01442350903069931
[5] S. Chakrabarty, M. Holz, E.K. Campbell, A. Banerjee, D. Gerlich and J.P. Maier, J. Phys. Chem. Lett. **4**, 4051 (2013). doi:10.1021/jz402264n
[6] X.B. Wang, H.K. Woo, B. Kiran and L.S. Wang, Angew. Chem. Int. Ed. **44**, 4968 (2005). doi:10.1002/anie.200501349
[7] X.B. Wang and L.S. Wang, Rev. Sci. Instrum. **79**, 073108 (2008). doi:10.1063/1.2957610
[8] X.B. Wang, H.K. Woo and L.S. Wang, J. Chem. Phys. **123**, 051106 (2005). doi:10.1063/1.1998787
[9] X.B. Wang, H.K. Woo, X. Huang, M.M. Kappes and L.S. Wang, Phys. Rev. Lett. **96**, 143002 (2006). doi:10.1103/PhysRevLett.96.143002
[10] X.B. Wang, H.K. Woo, J. Yang, M.M. Kappes and L.S. Wang, J. Phys. Chem. C. **111**, 17684 (2007). doi:10.1021/jp0703861
[11] X.B. Wang, K. Matheis, I.N. Ioffe, A.A. Goryunkov, J. Yang, M.M. Kappes and L.S. Wang, J. Chem. Phys. **128**, 114307 (2008). doi:10.1063/1.2889384
[12] C. Hock, J.B. Kim, M.L. Weichman, T.I. Yacovitch and D.M. Neumark, J. Chem. Phys. **137**, 244201 (2012). doi:10.1063/1.4772406
[13] M.L. Weichman and D.M. Neumark, Ann. Rev. Phys. Chem. **69**, 101 (2018). doi:10.1146/annurev-physchem-050317-020808
[14] H.T. Liu, C.G. Ning, D.L. Huang, P.D. Dau and L.S. Wang, Angew. Chem. Int. Ed. **52**, 8976 (2013). doi:10.1002/anie.201304695
[15] L.S. Wang, J. Chem. Phys. **143**, 040901 (2015). doi:10.1063/1.4927086
[16] G.Z. Zhu and L.S. Wang, Chem. Sci. **10**, 9409 (2019). doi:10.1039/C9SC03861B
[17] G.S. Kocheril, H.W. Gao, D.F. Yuan and L.S. Wang, J. Chem. Phys. **157**, 17110 (2022). doi:10.1063/5.0127877
[18] K.M. Ervin, J. Ho and W.C. Lineberger, J. Chem. Phys. **92**, 5405 (1988). doi:10.1021/j100330a017
[19] C. Xu, E. de Beer and D.M. Neumark, J. Chem. Phys. **104**, 2749 (1996). doi:10.1063/1.470983
[20] E.P.F. Lee, J.M. Dyke, F.-T. Chau, W.-K. Chow and D.K.W. Mok, Chem. Phys. Lett. **429**, 365 (2006). doi:10.1016/j.cplett.2006.08.063
[21] E.P.F. Lee, J.M. Dyke, F.-T. Chau, W.-K. Chow and D.K.W. Mok, J. Chem. Phys. **125**, 064307 (2006). doi:10.1063/1.2335445
[22] E.P.F. Lee, J.M. Dyke, D.K.W. Mok, F.-T. Chau and W.-K. Chow, J. Chem. Phys. **127**, 094306 (2007). doi:10.1063/1.2768355
[23] R.P. Kampf and J.M. Parson, J. Chem. Phys. **108**, 7595 (1998). doi:10.1063/1.476194
[24] B. Dick, Phys. Chem. Chem. Phys. **21**, 19499 (2019). doi:10.1039/C9CP03353J
[25] I. Leon, Z. Yang, H.T. Liu and L.S. Wang, Rev. Sci. Instrum. **85**, 083106 (2014). doi:10.1063/1.4891701
[26] J. Cooper and R.N. Zare, J. Chem. Phys. **48**, 942 (1968). doi:10.1063/1.1668742
[27] A. Sanov and R. Mabbs, Int. Rev. Phys. Chem. **27**, 53 (2008). doi:10.1080/01442350701786512
[28] R.E. March and J.F.J. Todd, *Quadrupole Ion Trap Mass Spectrometry*, 2d Ed (Wiley, Hoboken, New Jersey, 2005.
[29] S. Gozem and A.I. Krylov, Wiley Interdiscip. Rev.: Comput. Mol. Sci. **12**, e1546 (2021).
[30] H.T. Liu, C.G. Ning, D.L. Huang and L.S. Wang, Angew. Chem., Int. Ed. **53**, 2464 (2014). doi:10.1002/anie.201310323
[31] D.L. Huang, G.Z. Zhu and L.S. Wang, J. Chem. Phys. **142**, 091103 (2015). doi:10.1063/1.4913924
[32] G.Z. Zhu, Y. Liu and L.S. Wang, Phys. Rev. Lett. **119**, 023002 (2017). doi:10.1103/PhysRevLett.119.023002
[33] C.M. Western and J. Quant, Spectrosc. Radiat. Transf. **186**, 221 (2017). doi:10.1016/j.jqsrt.2016.04.010